Designing tie knots by random walks

The simplest of conventional tie knots, the four-in-hand, has its origins in late-nineteenth-century England. The Duke of Windsor, as King Edward VIII became after abdicating in 1936, is credited with introducing what is now known as the Windsor knot, from which its smaller derivative, the half-Windsor, evolved. In 1989, the Pratt knot, the first new knot to appear in fifty years, was revealed on the front page of *The New York Times*.

Rather than wait another half-century for the next sartorial advance, we have taken a more formal approach. We have developed a mathematical model of tie knots, and provide a map between tie knots and persistent random walks on a triangular lattice. We classify knots according to their size and shape, and quantify the number of knots in each class. The optimal knot in a class is selected by the proposed aesthetic conditions of symmetry and balance. Of the 85 knots that can be tied with a conventional tie, we recover the four knots that are in widespread use and introduce six new aesthetically pleasing knots.

A tie knot is started by bringing the wide (active) end to the left and either over or under the narrow (passive) end, dividing the space into right (R), centre (C) and left (L) regions (Fig. 1a). The knot is continued by subsequent half-turns, or moves, of the active end from one region to another (Fig. 1b) such that its direction alternates between out of the shirt ($\odot$) and into the shirt ($\otimes$). To complete a knot, the active end must be wrapped from the right (or left) over the front to the left (or right), underneath to the centre and finally through (denoted T but not considered a move) the front loop just made.

Elements of the move set $\{R_\odot, R_\otimes, C_\odot, C_\otimes, L_\odot, L_\otimes\}$ designate the moves necessary to place the active end into the corresponding region and direction. We can then define a tie knot as a sequence of moves initiated by $L_\otimes$ or $L_\odot$ and terminating with the subsequence $R_\odot L_\otimes C_\odot T$ or $L_\odot R_\otimes C_\odot T$. The sequence is constrained such that no two consecutive moves indicate the same region or direction.

We represent knot sequences as random walks on a triangular lattice (Fig. 1c). The axes *r, c* and *l* correspond to the three move regions R, C and L, and the unit vectors $\hat{\mathbf{r}}, \hat{\mathbf{c}}$ and $\hat{\mathbf{l}}$ represent the corresponding moves; we omit the directional notation $\odot, \otimes$ and the terminal action T. Because all knot sequences end with $C_\odot$ and alternate between $\odot$ and $\otimes$, all knots of odd numbers of moves begin with $L_\odot$, whereas those of even numbers of moves begin with $L_\otimes$.

Our simplified random-walk notation is therefore unique.

The size of a knot, and the primary parameter by which we classify it, is the number of moves in the knot sequence, denoted by the half-winding number *h*. The initial and terminal sequences dictate that the smallest knot is given by the sequence $L_\odot R_\otimes C_\odot T$, with $h = 3$. Practical considerations (namely the finite length of the tie), as well as aesthetic ones, suggest an upper bound on knot size, so we limit our exact results to $h \leqslant 9$.

The number of knots as a function of size, $K(h)$, corresponds to the number of walks of length *h* beginning with $\hat{\mathbf{l}}$ and ending with $\hat{\mathbf{r}}\hat{\mathbf{l}}\hat{\mathbf{c}}$ or $\hat{\mathbf{l}}\hat{\mathbf{r}}\hat{\mathbf{c}}$. It may be written
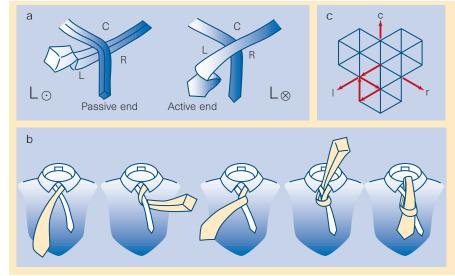
$$K(h) = (1/3)(2^{h-2} - (-1)^{h-2})$$

where $K(1) = 0$, and the total number of knots is $\sum_{i=1}^{9} K(i) = 85$.

The shape of a knot depends on the number of right, centre and left moves in the tie sequence. Because symmetry dictates that there be an equal number of right and left moves (see below), the shape of a knot is characterized by the number of centre moves γ. We use it to classify knots of equal size *h*; knots with identical *h* and γ belong to the same class. A large centre fraction γ/h indicates a broad knot (such as the Windsor) and a small centre fraction suggests a narrow one (such as the four-in-hand), but not all centre fractions allow aesthetic knots. We therefore limit our attention to $1/4 \leqslant \gamma/h \leqslant 1/2$.

The number of knots in a class, $K(h, \gamma)$, is equivalent to the number of walks of length *h* that satisfy the boundary conditions and contain γ steps $\hat{\mathbf{c}}$; it appears as

$$K(h, \gamma) = 2^{\gamma - 1} \binom{h - \gamma - 2}{\gamma - 1}$$

Figure 1 All diagrams are drawn in the frame of reference of the mirror image of the actual tie. **a,** The two ways of beginning a knot, $L_\odot$ and $L_\otimes$. For knots beginning with $L_\odot$, the tie must begin inside-out. **b,** The four-in-hand, denoted by the sequence $L_\otimes R_\odot L_\otimes C_\odot T$. **c,** A knot may be represented by a persistent random walk on a triangular lattice. The example shown is the four-in-hand, indicated by the walk $\hat{\mathbf{l}}\hat{\mathbf{r}}\hat{\mathbf{l}}\hat{\mathbf{c}}$.

Table 1 Aesthetic tie knots

h	γ	γ/h	K(h, γ)	s	b	Name	Sequence
3	1	0.33	1	0	0		$L_\odot R_\otimes C_\odot T$
4	1	0.25	1	−1	1	Four-in-hand	$L_\otimes R_\odot L_\otimes C_\odot T$
5	2	0.40	2	−1	0	Pratt knot	$L_\odot C_\otimes R_\odot L_\otimes C_\odot T$
6	2	0.33	4	0	0	Half-Windsor	$L_\otimes R_\odot C_\otimes L_\odot R_\otimes C_\odot T$
7	2	0.29	6	−1	1		$L_\odot R_\otimes L_\odot C_\otimes R_\odot L_\otimes C_\odot T$
7	3	0.43	4	0	1		$L_\odot C_\otimes R_\odot C_\otimes L_\odot R_\otimes C_\odot T$
8	2	0.25	8	0	2		$L_\otimes R_\odot L_\otimes C_\odot R_\otimes L_\odot R_\otimes C_\odot T$
8	3	0.38	12	−1	0	Windsor	$L_\otimes C_\odot R_\otimes L_\odot C_\otimes R_\odot L_\otimes C_\odot T$
9	3	0.33	24	0	0		$L_\odot R_\otimes C_\odot L_\otimes R_\odot C_\otimes L_\odot R_\otimes C_\odot T$
9	4	0.44	8	−1	2		$L_\odot C_\otimes R_\odot C_\otimes L_\odot C_\otimes R_\odot L_\otimes C_\odot T$

Knots are characterized by half-winding number *h*, centre number γ, centre fraction γ/h, knots per class $K(h, \gamma)$, symmetry *s*, balance *b*, name and sequence.

The symmetry of a knot, which is our first aesthetic constraint, is determined by the number of moves to the right minus the number of moves to the left,

$$s = \sum_{i=1}^{h} x_i$$

where $x_i = 1$ if the ith step is $\hat{\mathbf{r}}$, -1 if the ith step is $\hat{\mathbf{l}}$ and 0 otherwise. Because asymmetric knots disrupt human bilateral symmetry, we consider the most symmetric knots from each class, that is, the ones that minimize s.

Whereas the centre number γ and the symmetry s specify the move composition of a knot, balance relates to the distribution of these moves; it corresponds to the extent to which the moves are mixed. A balanced knot is tightly bound and keeps its shape. We use this as our second aesthetic constraint. The balance b may be expressed as

$$b = (1/2) \sum_{i=2}^{h-1} |\omega_i - \omega_{i-1}|$$

and the winding direction $\omega_i(\sigma_i, \sigma_{i+1}) = 1$, where σ_i represents the ith step of the walk, if the transition from σ_i to σ_{i+1} is clockwise, say, and -1 otherwise. Of those knots that are optimally symmetric, we desire that knot which minimizes b.

The ten canonical knot classes $\{h, \gamma\}$ and the corresponding most aesthetic knots are listed in Table 1. The four named knots are the only ones, to our knowledge, to have received widespread attention, either published or through tradition. Here we introduce some unnamed knots.

The first four columns of Table 1 describe the knot class $\{h, \gamma\}$, whereas the remainder relate to the corresponding most aesthetic knot. The centre fraction γ/h provides a guide to the shape of a knot, with higher fractions corresponding to broader knots; along with the size h, it should be used in selecting a knot.

Some readers may notice the use of knots whose sequences are equivalent to those shown in Table 1 apart from transpositions of $\hat{\mathbf{r}}$, $\hat{\mathbf{l}}$ groups, such as the use of $L_\otimes R_\odot C_\otimes R_\odot L_\otimes C_\odot T$ in place of the half-Windsor (T. P. Harte and L. S. G. E. Howard, personal communication); some will argue that this *is* the half-Windsor. Such ambiguity follows from the variable width of conventional ties (the earliest ties were uniformly wide). This makes some transpositions arguably favourable, namely the last $\hat{\mathbf{r}}$, $\hat{\mathbf{l}}$ group in the knots $\{5, 2\}$, $\{6, 2\}$, $\{7, 2\}$, $\{8, 3\}$ and $\{9, 3\}$ in Table 1. We do not attempt to distinguish between these knots and their counterparts; this much we leave to the sartorial discretion of the reader.

Thomas M. Fink, Yong Mao
Cavendish Laboratory,
Cambridge CB3 0HE, UK
e-mail: tmf20@cus.cam.ac.uk

Pasture damage by an Amazonian earthworm

Almost all cultivated soils undergo some reduction in the porosity of the surface layers, and nowhere is this more evident than in tropical rainforests that have been converted to pastures. Following deforestation in an area of Costa Rica, soil bulk density has been shown to increase rapidly after conversion to pasture, leading to poor drainage and a reduced rate of gaseous diffusion[1]. These factors limit methane consumption and promote the anaerobic production of methane. A similar effect on methane flux has been found in upland soils in the Brazilian Amazonian basin after conversion from forest to pasture[2,3]. Increases in atmospheric methane are therefore not limited to emissions from flooded soils[4], as forest-to-pasture conversion promotes the anaerobic mineralization of organic matter by changing the physical properties of soil.

We now demonstrate the importance of this process in pasture degradation in central Amazonia, close to Manaus in northern Brazil (Fig. 1a). We show that, in addition to the substantial compacting effects of heavy machinery[5] and cattle trampling[6], another more insidious agent — the soil macrofauna — can have profound and lasting effects[7,8] on the porosity of pasture soils.

We wetted a natural forest soil (xanthic acrudox, USDA, 1996) to a water potential of -10 kPa and compressed it at a pressure of 10^3 kPa, measured using an oedometer. Macroporosity (in the range 0.1. to 100 μm) fell from 21.7 to 3 cm^3 per 100 g, indicating that forest surface soils (at a depth of 0–5 cm) are extremely sensitive to compaction (Fig. 1b). Passing the same soil through the gut of the earthworm *Pontoscolex corethrurus*, an aggressive exotic colonist that invades many tropical pastures, reduced macroporosity even more to 1.6 cm^3 per 100 g. We believe that this change is brought about by the intense mixing and near-complete dispersion of soil particles in the moist environment of the earthworm gut (water content: 0.85 g per g).

During conversion from forest to pasture, two separate mechanisms act to compact the soil. First, the effects of heavy machinery[5] and trampling by cattle[6] occur in specific locations and result from the techniques used for deforestation and pasture management. They lead to the mixing of plant debris and clay in the upper 5 cm and to severe compaction in the layer 5–10 cm deep (Fig. 1c). Second, the effects of reduced abundance and diversity of macrofaunal communities in the newly created pastures are linked to ecosystem dynamics
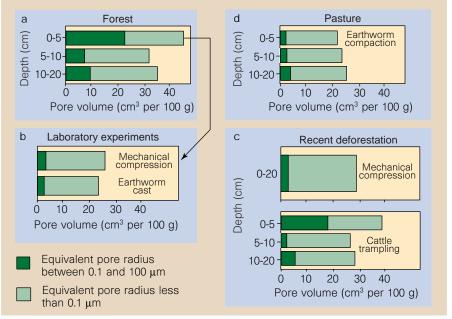

Figure 1 Effect of mechanical and biological action on soil pore distribution in central Amazonia. Data are deduced from mercury porosimetry analysis[10]. The pore size distribution shows a bimodal pattern, indicating that there are two types: the largest pores, which have an equivalent pore radius (EPR) between 0.1 and 100 μm, are biological in origin or are fine fissures, and are essential for gas exchange and the infiltration and retention of free water; the smaller pores, with an EPR of less than 0.1 μm, are found in compact clumps of kaolinite. **a,** In primary forest, biodiverse soil macrofauna and roots regulate soil pore volume. **b,** Laboratory experiments in which the forest surface horizon is compacted by mechanical compression (10^3 kPa) of soil with a water potential of -10 kPa, or by mechanical working and dispersion in the earthworm gut. **c,** Effects of recent deforestation due to heavy machinery and trampling by cattle (after manual clearance). **d,** Ungrazed, manually deforested pasture shows accumulation of compact surface casts in the layer 0–5 cm deep.